On-chip supercapacitors with ultrahigh volumetric performance based on electrochemically co-deposited CuO/polypyrrole nanosheet arrays

2015 Nanotechnology 26 425402

(http://iopscience.iop.org/0957-4484/26/42/425402)

IOP Publishing Nanotechnology
Nanotechnology **26** (2015) 425402 (8pp) doi:10.1088/0957-4484/26/42/425402

On-chip supercapacitors with ultrahigh volumetric performance based on electrochemically co-deposited CuO/polypyrrole nanosheet arrays

Tao Qian[1,3], Jinqiu Zhou[1,3], Na Xu[1], Tingzhou Yang[1], Xiaowei Shen[1], Xuejun Liu[1], Shishan Wu[2] and Chenglin Yan[1]

[1] College of Physics, Optoelectronics and Energy & Collaborative Innovation Center of Suzhou Nano Science and Technology, Soochow University, No.1 Shizi Street, Suzhou 215006, People's Republic of China
[2] School of Chemistry and Chemical Engineering, Nanjing University, Nanjing, 210093, People's Republic of China

E-mail: c.yan@suda.edu.cn

Received 2 July 2015, revised 22 August 2015
Accepted for publication 1 September 2015
Published 30 September 2015

Abstract

We introduce a new method for fabricating unique on-chip supercapacitors based on CuO/polypyrrole core/shell nanosheet arrays by means of direct electrochemical co-deposition on interdigital-like electrodes. The prepared all-solid-state device demonstrates exceptionally high specific capacitance of 1275.5 F cm^{-3} (~40 times larger than that of CuO-only supercapacitors) and high-energy-density of 28.35 mWh cm^{-3}, which are both significantly greater than other solid-state supercapacitors. More importantly, the device maintains approximately 100% capacity retention at 2.5 A cm^{-3} after 3000 cycles. The *in situ* co-deposition of CuO/polypyrrole nanosheets on interdigital substrate enables effective charge transport, electrode fabrication integrity, and device integration. Because of their high energy, power density, and stable cycling stability, these newly developed on-chip supercapacitors permit fast, reliable applications in portable and miniaturized electronic devices.

S Online supplementary data available from stacks.iop.org/NANO/26/425402/mmedia

Keywords: on-chip energy storage, CuO, energy

(Some figures may appear in colour only in the online journal)

1. Introduction

As the global economy is rapidly developing and the human population is growing, tremendous research efforts have been devoted to energy storage because of the increasing demand for energy in the new century [1–5]. The supercapacitor is a promising energy storage device because of its high power density, rapid charge/discharge rate, long cycle life, and low maintenance cost. Recently, miniaturized solid-state energy storage devices, which enable designers to place energy storage devices directly on a chip, have become one of the most intense research focuses in the field of electrical energy storage [6, 7]. A flexible electrode with favorable mechanical strength and large capacitance is a vital component for flexible supercapacitors. However, it still remains a challenging task to fabricate supercapacitor electrodes that are lightweight, flexible, and high performance for flexible and on-chip energy storage devices.

Two main working principles are established for supercapacitors. The first is electrochemical double-layer charge

[3] The first two authors contributed equally to this work.

storage through which carbon-based materials can work. Xuebin Wang *et al* [8] and Xiaowei Yang *et al* [9] describe advanced carbon-based materials with high energy/power density for supercapacitors. The second is pseudocapacitive charge storage, which includes rapid redox reactions at the surface and bulk of the electrodes, through which conducting polymer and transition metal oxide-based materials can work [10–12]. For pseudocapacitors, properties such as high specific surface area, electrical conductivity, and a fast cation diffusion process are important to achieve high power density and energy density. Ruthenium oxides and hydroxides have been previously demonstrated to show very high pseudocharge capacitance [13, 14]. Of course, other transition metal oxides were also well studied, for example, NiO, CoO, MnO_x, and WO_x, SnO_2 [15–25]. Among these metal oxides, copper-based materials such as copper oxides and hydroxides are attractive and promising pseudocapacitive electrode materials because of their chemical stability, low cost, and environmental friendliness. To the best of our knowledge, little research has been conducted on the application of CuO as on-chip supercapacitor electrodes because of their low electrical conductivity and unstable cycling performances [26, 27, 30, 33, 35–37]. Polypyrrole (PPy) is an intrinsically conductive polymer because of its high conductivity, storage ability, redox and capacitive current, and good thermal and environmental stability [18, 28, 29]. Its high electrical conductivity with respect to that of copper oxide will certainly result in significantly improved electron transport. In this paper, we constructed an on-chip, flexible, all-solid-state supercapacitor based on a CuO/PPy nanosheet array through direct electrochemical co-deposition on interdigital-like copper substrates, which are compatible with current microelectronics. The results reveal that the prepared nanosheets that are integrated firmly and uniformly with the pre-patterned copper substrate significantly improve the conductivity of copper oxide and lead to a high specific capacitance of 1275.5 F cm^{-3} at a current density of 2.5 A cm^{-3} with 100% capacity retention. Moreover, the specific capacitance of the hybrid CuO/PPy device is ~40 times larger than that of the CuO-only devices. The extreme high performance is attributed to the smart synergetic contribution from the CuO/PPy core/shell nanosheets.

2. Experimental methods

2.1. Synthesis of the CuO/PPy nanosheet arrays on the interdigital-like copper substrate

We prepared a 10 mg mL^{-1} graphene dispersion with 0.1 M pyrrole (purchased from Sinopharm Chemical Reagent Co., Ltd) and 0.1 M sodium dodecyl sulfate (SDS, purchased from ChinaSun Specialty Products Co., Ltd). The copper substrate patterned on polyethylene terephthalat (PET, $2 \times 3\ cm^2$, figure 1) served as the working electrode, an Ag/AgCl electrode served as reference electrode, and a platinum wire as counter electrode. Next, the electrochemical co-deposition was carried out through method of cyclic voltammetry (CV) in a potential range of $-1.2 \sim 0.8$ V at a scan rate of 20 mV s^{-1}. Finally, the product was washed by deionized water several times and dried in room air.

2.2. Fabrication of an all-solid-state flexible supercapacitor

The flexible all-solid-state supercapacitor was manufactured by means of the usual procedure: 6 g (Polyvinyl Alcohol) PVA was added into 50 mL deionized water with continuous stirring at 90 °C. After the PVA was dissolved completely, 4 g KOH in 10 mL water was added [33]. Two branches of the obtained product were covered by the gel electrolyte with the same size.

2.3. Characterization of the CuO/PPy nanosheets

The morphology of the hybrid nanosheets was observed by field emission scanning electron microscopy (FESEM, SU8010, Japan), and field emission transmission electron microscopy (FETEM, FEI Tecnai G2 F20 S-TWIN TMP, Hongkong). X-ray photoelectron spectroscopy (XPS) measurements were performed on a PHI 5000 VersaProbe.

2.4. Electrochemical measurements of the supercapacitor

Supercapacitor performance of the prepared device was investigated by using CV and galvanostatic charge/discharge experiments. A three-electrode configuration with a prepared product working electrode, a platinum wire counter electrode, and an Ag/AgCl reference electrode was used for the electrochemical impedance spectroscopy (EIS) measurement with a frequency range of 100 kHz to 10 mHz in a 6 M KOH solution. All the measurements were recorded by a CHI 660E (Chenhua Shanghai, China) electrochemical workstation.

3. Results and discussion

3.1. Physical characterization

Simplified schematic images of the fabrication process of on-chip and all-solid-state supercapacitor based on CuO/PPy nanosheet arrays are illustrated in figure 1. Before co-deposition, 2 four-interdigital-finger copper substrate electrodes were patterned on-chip. After co-deposition, the electrodes became black with hybrid CuO/PPy nanosheets selectively grown on the interdigital fingers. Each finger has a length of 13 mm, a width of 1 mm, and an interelectrode distance of 1 mm.

The structure of the CuO/PPy core/shell nanosheets grown on the interdigital-like copper substrate electrode of the prepared supercapacitor is clearly illustrated in figures 2(A)–(C). To investigate the morphology of the CuO/PPy nanosheets after electrochemical co-deposition, scanning electron microscopy (SEM), and high-resolution transmission electron microscopy (HRTEM) were carried out and the results are shown in figure 2. SEM images reveal the prepared nanosheets integrated firmly and uniformly with the interdigital-like copper substrate (figures 2(D) and S1). A core/

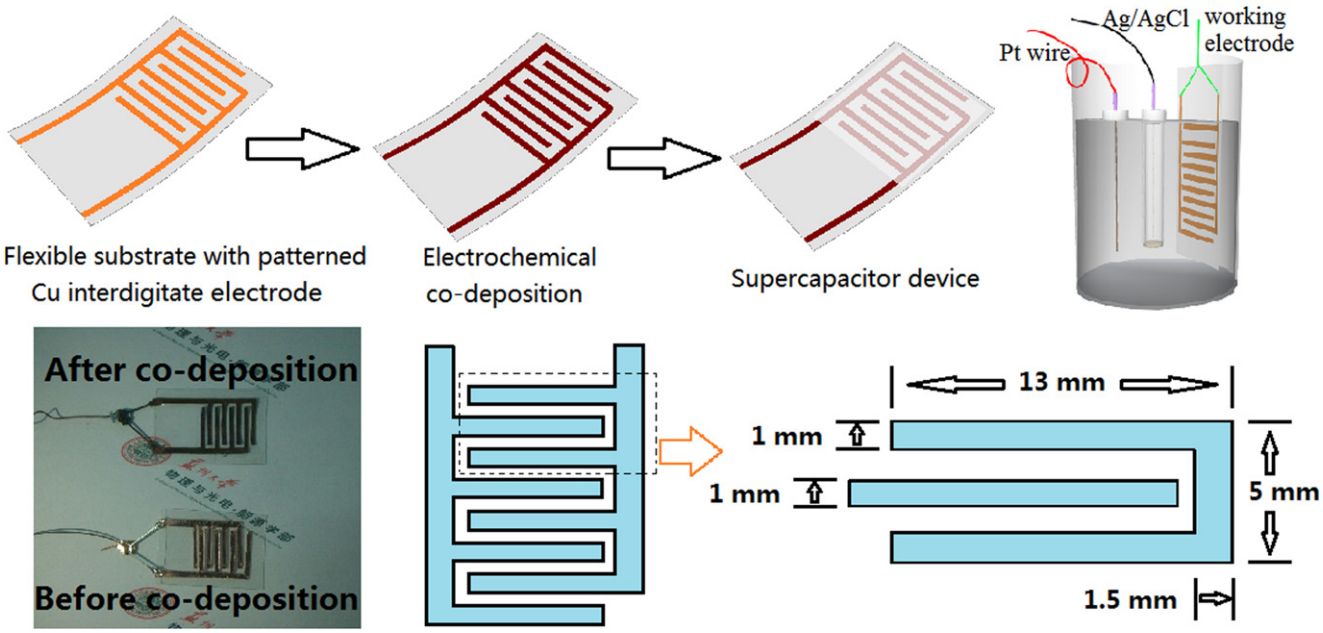

Figure 1. Schematics of the fabrication process of flexible all-solid-state supercapacitors based on CuO/PPy nanosheet arrays and the detailed parameters for the designed electrodes.

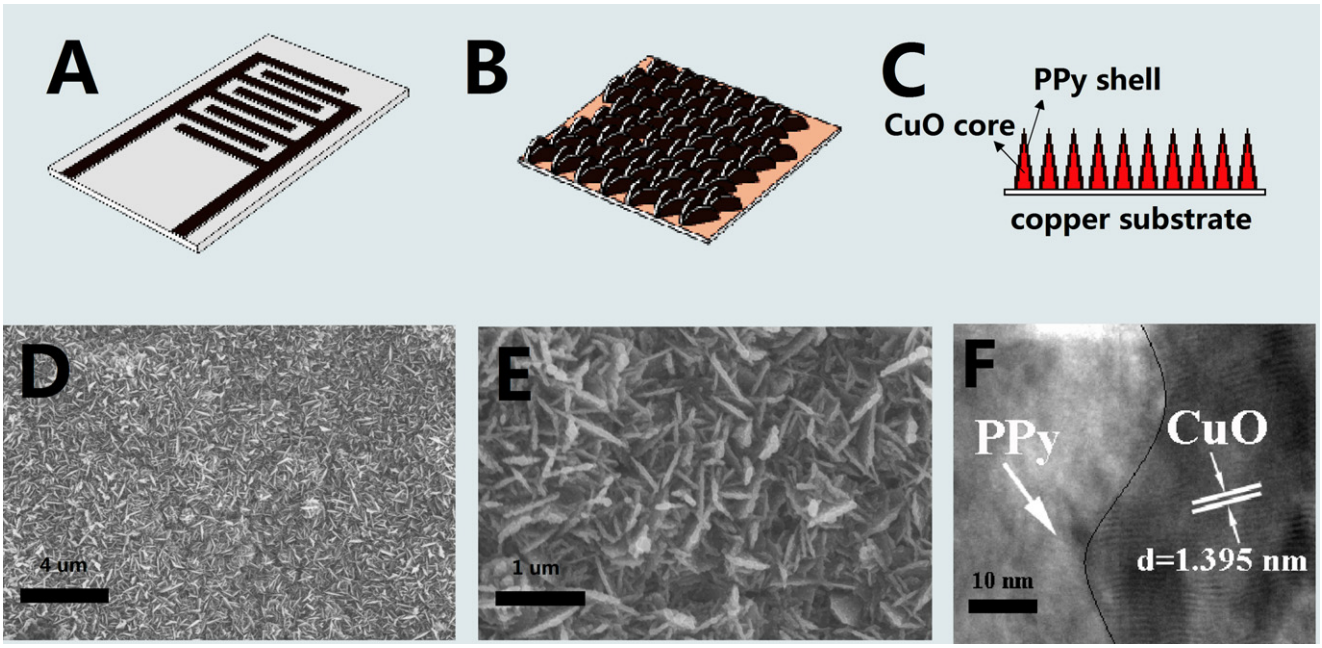

Figure 2. (A) Schematics of the prepared supercapacitor. (B) Illustration of the prepared nanosheet arrays on interdigital-like copper substrates by partially enlarged view. (C) Cross-section of the core shell nanosheets. (D) Low-magnification and (E) high-magnification SEM images of the hybrid nanosheets. (F) HRTEM image of a magnified view of the resulting nanosheet showing the CuO crystal lattice and amorphous PPy structures.

shell structure could be clearly observed in figure 2(E) with a rough surface of coated PPy layers. These structures are further confirmed by the detailed morphology in the HRTEM image. The core/shell structure with highly crystalline CuO core and amorphous PPy shell can be clearly identified, as shown in figure 2(F).

To examine the chemical composition, we performed the XPS measurement of the CuO/PPy nanosheets, as shown in figure 3(A). In the survey region from 200 to 1000 eV, it is evident that C, O, and Cu elements all exist in the sample. The peaks at 932.3 and 952.2 eV are assigned to the binding energy of $Cu2p_{3/2}$ and $Cu2p_{1/2}$, respectively, indicating the presence of Cu in the sample. The difference between them is found to be ~10 eV, further justifying the existence of CuO in the sample. Additionally, two satellite peaks observed at 943.5 and 962.6 eV, which are positioned at higher binding energies compared to the main peaks, confirm that the oxide in the sample is CuO [30]. The high-resolution spectrum of

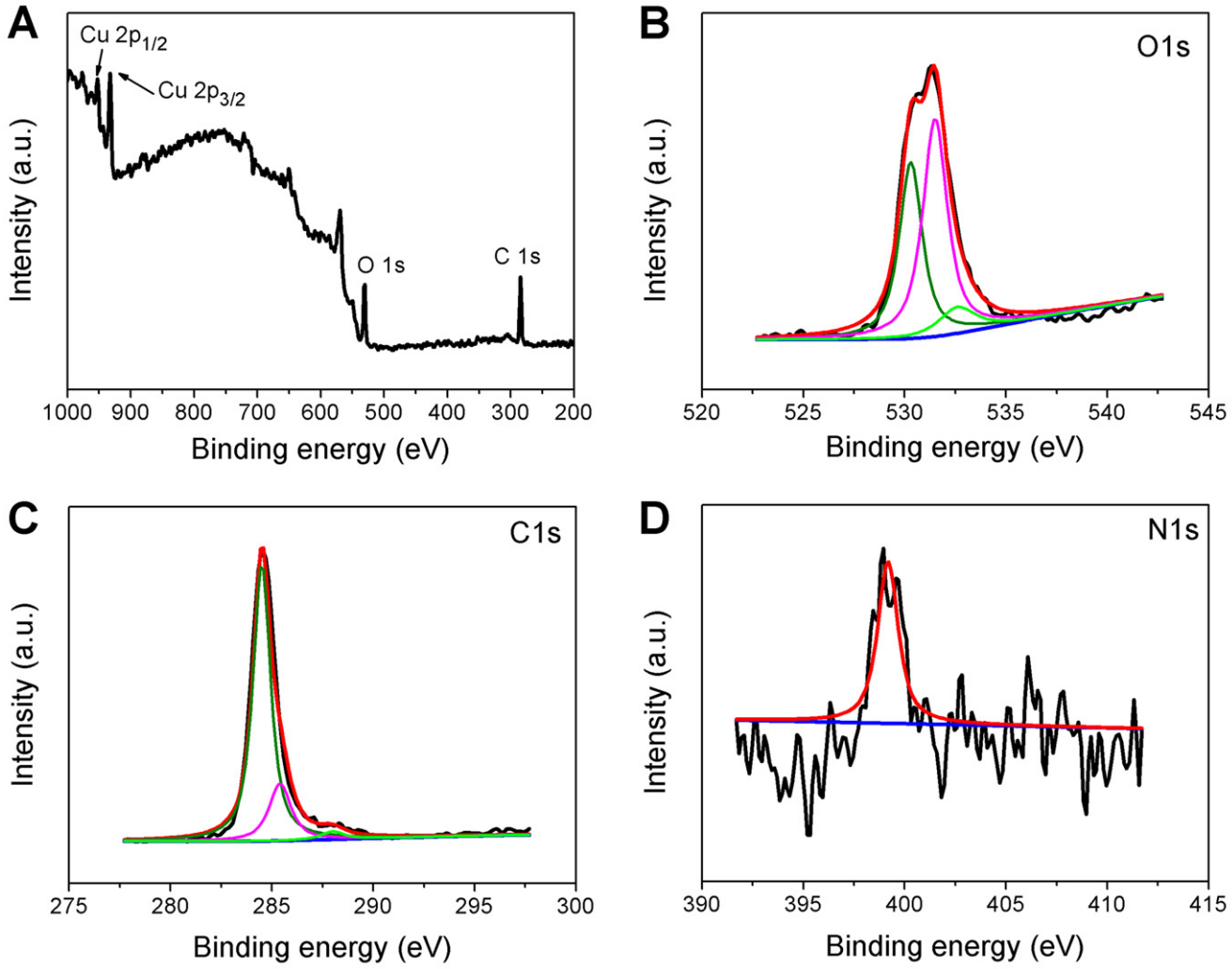

Figure 3. XPS spectra of the CuO/PPy nanosheets (A) Full XPS spectra and the high resolution (B) O1s, (C) C1s and (D) N1s XPS spectrum.

O1s in figure 3(B) shows a curve which can be fit to three peaks with binding energies at 530.3, 531.5, and 532.6 eV. The two peaks at 530.3 and 531.5 eV are attributed to the oxygen in CuO and $Cu(OH)_2$, respectively. The XPS peak at 532.6 eV corresponds to the water molecule, indicating that the CuO nanosheets are in hydrated form [31]. The high-resolution C1s of the sample (figure 3(C)) is clearly divided into three components at 284.5, 285.4, and 288.0 eV corresponding to C-C, C-N, and C=O [32]. C-N indicates the existence of PPy. From figure 3(D), it can be seen that the only peak at 399.2 eV corresponds to N atoms, which further justifies the presence of PPy.

3.2. Electrochemical characterization

The electrochemical properties of the supercapacitor were investigated by CV, galvanostatic charge/discharge, and EIS. The *CV* curves in the potential range of $0 \sim 0.4$ V at different scan rates (figure 4(A)) show well-resolved pairs of cathodic and anodic peaks which are very distinct from those of the electric double-layer capacitance which is normally close to an ideal rectangular shape. The current of the electrode responses quasi-linearly with increasing potential scan rate, demonstrating its excellent reactivity [33]. Plots of the galvanostatic charge/discharge voltage vs. the time were measured with the voltage window of $0 \sim 0.4$ V at current densities of 2.5, 3.5, 5.0, 7.5, 10.0 A cm^{-3} (figure 4(B)). We observed well-defined plateaus during the discharge processes, revealing their satisfactory pseudocapacitive behavior. The volumetric capacitance (C_V) of the device was calculated by the following equation:

$$C_v = I\Delta t / V\Delta E \quad (1)$$

where I is the discharge current, Δt is the discharge time, ΔE is the potential window during the discharge process, and V is the effective electrode volume [34]. The calculated volumetric capacitance of the prepared supercapacitor was 1275.5 F cm^{-3} at a current density of 2.5 A cm^{-3}, which is about 40 times larger than that of CuO-only device (only 31.25 F cm^{-3} as shown in figure S4). In comparison with other advanced electrode materials, the capacitor property in this work is much greater than those of the other solid-state or solution

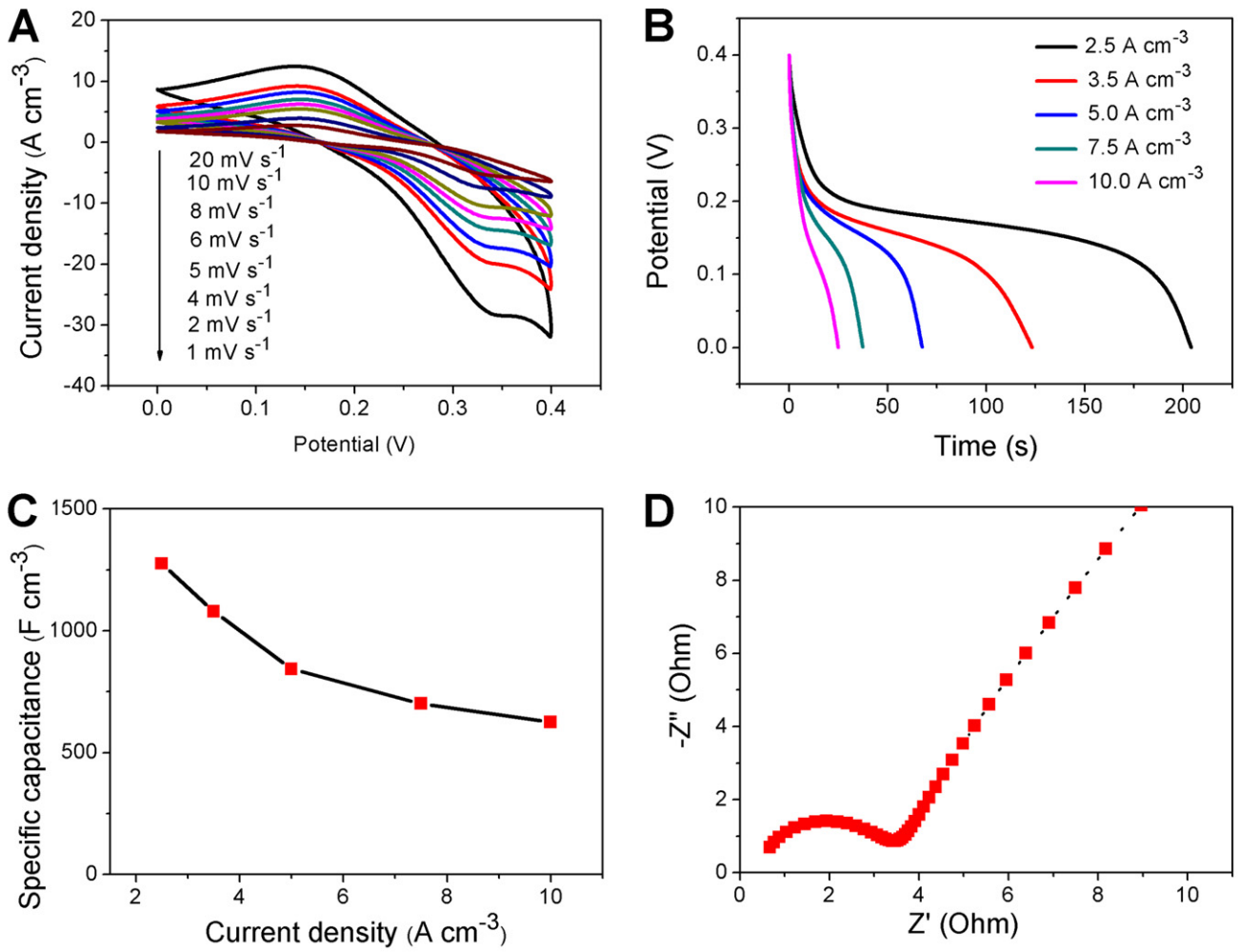

Figure 4. Electrochemical characterization: (A) *CV* curves of the prepared supercapacitor in a potential range of 0 ∼ 0.4 V at scan rates of 20, 10, 8, 6, 5, 4, 2, 1 mV s^{-1}. (B) Galvanostatic charge/discharge curves of the prepared supercapacitor device at current densities of 2.5, 3.5, 5.0, 7.5, 10.0 A cm^{-3}. (C) Volumetric capacitance at different current densities. (D) Nyquist plot of the prepared CuO/PPy nanosheet arrays electrode.

Table 1. The comparison results of different capacitor electrode materials for the supercapacitors.

Capacitor materials	Specific capacitance (F cm^{-3})	References
Aligned nano-porousgraphite oxide	177	[39]
N and B co-doped graphene	488	[40]
3-D nanoporous NiF_2-dominant thin film	733	[41]
Hierarchically structured CNT-graphene fibres	300	[42]
polyaniline nanowire arrays	588	[29]
On-chip CuO/PPy supercapacitors	**1275.5**	**This work**

based supercapacitors (table 1). Notably, the capacitance was calculated to be 625 F cm^{-3} even at a discharge current density of 10.0 A cm^{-3} (figure 4(C)), suggesting the excellent capacitor properties of the such on-chip supercapacitors.

EIS measurement in the frequency range of 10 mHz to 10 kHz was performed to clearly understand the ion diffusion of the electrodes. The Nyquist plot (figure 4(D)) shows a form with a semicircle at higher frequency region and a spike at lower frequency which is a characteristic of the capacitive behavior. At the high frequency, the intersection of the curve at the real part represents the resistance of the electrochemical system ($R_s \sim 0.2\,\Omega$ including the inherent resistance of the electroactive material, ionic resistance of electrolyte, and contact resistance at the interface between electrolyte and electrode) and the semicircle diameter reflects the charge-transfer resistance ($R_{ct} \sim 4\,\Omega$). The straight line indicates the diffusion of the electroactive species and a larger slope signifies more rapid diffusion [35]. We conclude that the prepared electrode has low charge-transfer resistance and ion-diffusion resistance, corresponding to a much increased

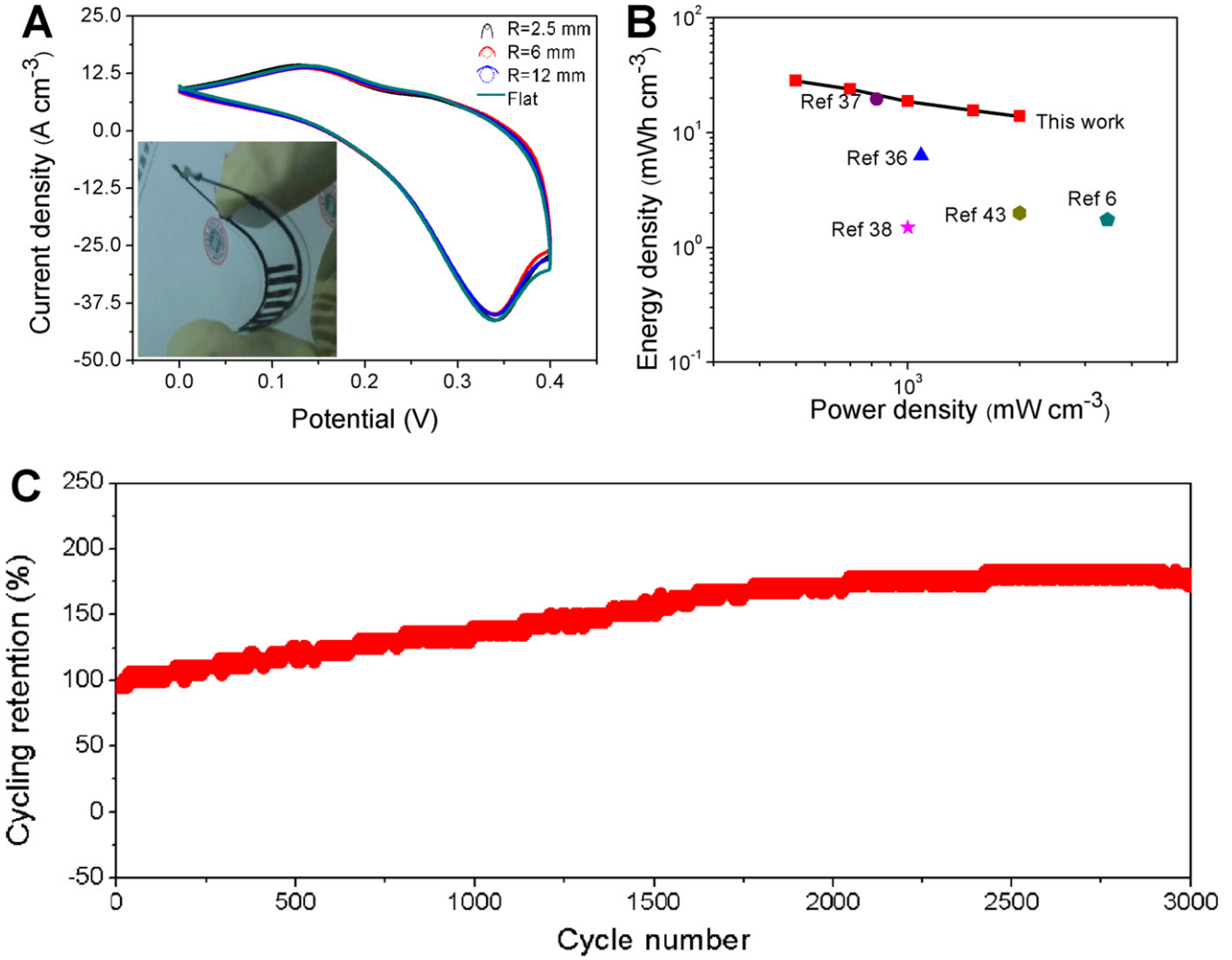

Figure 5. (A) Cyclic voltammetry curves measured at different bending states. The insert is the image of flexible supercapacitors. (B) Ragone plots of the prepared device and reportedsupercapacitors in the references. (C) The cycle performance of the prepared Cu/PPy electrode.

conductivity, which is beneficial for the rate capability enhancement.

To demonstrate the mechanical flexibility, *CV* measurement was conducted at a scan rate of 20 mV s^{-1}, with devices under various bending states (figure 5(A)). It is shown that the *CV* curves of the prepared supercapacitor measured with curvature radius ranging from 2.5 to 12 mm and without strain all show similar capacitive behavior with no capacitance decay, indicating the high flexibility of the as-prepared supercapacitors.

Energy density (E) and power density (P) are two key factors for evaluating the application of supercapacitors [8, 9], which can be calculated as

$$E = CV^2/2U \quad (2)$$

$$P = E/t \quad (3)$$

where C is total capacitance of the device, V is the cell voltage, U is the effective electrode volume, and t is the discharge time [34]. A power density of 500 mW cm^{-3} and an energy density of 28.35 mWh cm^{-3} were achieved at a current density of 2.5 A cm^{-3} (figure 5(B)), which are much higher than most of the reported supercapacitors in the references [6, 36–38, 43].

The cycling stability performance of the prepared supercapacitor was tested using the galvanostatic charge/discharge technique at a current density of 10.0 A cm^{-3}. Figure 5(C) shows the specific capacitance retention as a function of cycle number, indicating the increase trend of the specific capacitance during the initial 500 cycles, which is attributed to the gradual increase of the electrochemically active surface area. This phenomenon is due to the incomplete exposure of active materials to the gel electrolyte [44–46]. After 500 cycles, the capacitance increases slowly and trends to stabilization.

4. Conclusion

In conclusion, a new method of using direct co-deposition method on interdigital-like electrode was developed for the manufacture of on-chip supercapacitors based on CuO/PPy core/shell nanosheets. The prepared flexible all-solid-state

supercapacitor was found to exhibit superior performance in terms of specific capacitance, energy density, and power density. These results indicated that such CuO/PPy core/shell nanosheets could be considered as promising electrode materials for pseudocapacitor applications, especially for developing completely flexible pseudocapacitors using solid polymer electrolytes. In our work, the rationally designed on-chip supercapacitors allow the supercapacitor to be integrated with semiconductors, to meet the urgent demand for micro-scale energy storage devices.

Acknowledgments

This work was financially supported by the 'Thousand Talents Program', the Natural Science Foundation of Jiangsu Province of China (no. BK20140315), the National Natural Science Foundation of China (no. 51402202), the National Basic Research Program of China (no. 2015CB358600), the JiangsuShuangchuang Planand the Priority Academic Program Development of Jiangsu Higher Education Institutions (PAPD).

C Y and T Q conceived and coordinated the research. J Z, N X, and S W contributed to the synthesis, structural and electrochemical characterization. The manuscript was primarily written by J Z, T Q, and C Y, N X, T Y, X S, and X L contributed to discussions and manuscript review. All authors have given approval to the final version of the manuscript.

References

[1] Miller J R and Simon P 2008 Electrochemical capacitors for energy management *Science* **321** 651–2
[2] Simon P and Gogotsi Y 2008 Materials for electrochemical capacitors *Nat. Mater.* **7** 845–54
[3] Wang Y and Cao G Z 2008 Developments in nanostructured cathode materials for high-performance lithium-ion batteries *Adv. Mater.* **20** 2251–69
[4] Gogotsi Y and Simon P 2011 True performance metrics in electrochemical energy storage *Science* **334** 917–8
[5] Arico A S, Bruce P, Scrosati B, Tarascon J M and VanSchalkwijk W 2005 Nanostructured materials for advanced energy conversion and storage devices *Nat. Mater.* **4** 366–71
[6] Si W P, Yan C L, Chen Y, Oswald S, Han L Y and Schmidt O G 2013 All solid-state and flexible micro-supercapacitors with high performance based on MnO_x/Au multilayers *Energy Environ. Sci.* **6** 3218–23
[7] Wang K, Zou W J, Quan B G, Yu A F, Wu H P, Jiang P and Wei Z X 2011 All-state flexible micro-supercapacitor on a chip *Adv. Energy Mater.* **1** 1068–72
[8] Wang X B *et al* 2013 Three-dimensional strutted graphene grown by substrate-free sugar blowing for high-power-density supercapacitors *Nat. Commun.* **4** 2905
[9] Yang X W, Cheng C, Wang Y F, Qiu L and Li D 2013 Liquid-mediated dense integration of graphene materials for compact capacitive energy storage *Science* **341** 534–7
[10] Zhang L L and Zhao X S 2009 Carbon-based materials as supercapacitor electrode *Chem. Soc. Rev.* **28** 2520–31
[11] Péan C, Merlet C, Rotenberg B, Madden P A, Taberna P L, Daffos B, Salanne M and Simon P 2014 On the dynamics of charging in nanoporous carbon-based supercapacitors *ACS Nano* **2** 1576–83
[12] Yan J, Wang Q, Wei T and Fan Z J 2013 Recent advances in design and fabrication of electrochemical supercapacitors with high energy densities *Adv. Energy Mater.* **10** 1002–44
[13] Chang K H, Hu C C and Chou C Y 2007 Textural and capacitive characteristics of hydrothermally derived $RuO_{23}{\cdot}xH_2O$ nanocrystallites: independent control of crystal size and water content *Chem. Mater.* **1** 2112–9
[14] Hu C C, Chang K H, Lin M C and Wu Y T 2006 Design and tailoring of the nanotubular arrayed architecture of hydrous RuO_2 for next generation supercapacitors *Nano Lett.* **6** 2690–5
[15] Son J Y, ShinY H, Kim H J and Jang H M 2010 NiO resistive random access memory nanocapacitor array on graphene *ACS Nano* **4** 2655–8
[16] Ji J Y, Zhang L L, Ji H X, Li Y, Zhao X, Bai X, Fan X B, Zhang F B and Ruoff R S 2013 Nanoporous $Ni(OH)_2$ thin film on 3D ultrathin-graphite foam for asymmetric supercapacitor *ACS Nano* **7** 6237–43
[17] Dong X L, Guo Z Y, Song Y F, Hou M Y, Wang J Q, Wang Y G and Xia Y Y 2014 Flexible and wire-shaped micro-supercapacitor based on $Ni(OH)_2$-nanowire and ordered mesoporous carbon electrodes *Adv. Funct. Mater.* **24** 3405–12
[18] Zhou C, Zhang Y W, Li Y Y and Liu J P 2013 Construction of high-capacitance 3D CoO@Polypyrrole nanowire array electrode for aqueous asymmetric supercapacitor *Nano Lett.* **13** 2078−2085
[19] Zou W Y, Wang W, He B L, Sun M L and Yin Y S 2010 Supercapacitive properties of hybrid films of manganese dioxide and polyaniline based on active carbon in organic electrolyte *J. Power Sources* **195** 7489–93
[20] Xu C L, Zhao Y Q, Yang G W, Lia F S and Li H L 2009 Mesoporous nanowire array architecture of manganese dioxide for electrochemical capacitor applications *Chem. Commun.* **48** 7575–7
[21] Long J W, Sassin M B, Fischer A E and Rolison D R 2009 Multifunctional MnO_2-carbon nanoarchitectures exhibit battery and capacitor characteristics in alkaline electrolytes *J. Phys. Chem.* C **113** 17595–8
[22] Peng L L, Peng X, Liu B R, Wu C Z, Xie Y and Yu G H 2013 Ultrathin two-dimensional MnO_2/graphene hybrid nanostructures for high-performance, flexible planar supercapacitors *Nano Lett.* **13** 2151–7
[23] Tian Y Y, Cong S, Su W M, Chen H Y, Li Q W, Geng F X and Zhao Z G 2014 Synergy of $W_{18}O_{49}$ and polyaniline for smart supercapacitor electrode integrated with energy level indicating functionality *Nano Lett.* **14** 2150–6
[24] Wang H L, Cui L F, Yang Y, Casalongue H S, Robinson O T, Liang Y Y, Cui Y and Dai H J 2010 Mn_3O_4–graphene hybrid as a high-capacity anode material for lithium ion batteries *J. Am. Chem. Soc.* **132** 13978–80
[25] Deng J W, Yan C L, Yang L C, Baunack S, Oswald S, Wendrock H, Mei Y F and Schmidt O G 2013 Sandwich-stacked SnO_2/Cu hybrid nanosheets as multichannel anodes for lithium ion batteries *ACS Nano* **8** 6948–54
[26] Zhang X J, Shi W H, Zhu J X, Kharistal D J, Zhao W Y, Lalia B S, Hng H H and Yan Q Y 2011 High-power and high-energy-density flexible pseudocapacitor electrodes made from porous CuO nanobelts and single-walled carbon nanotubes *ACS Nano* **5** 2013–9
[27] Liu Y, Ying Y L, Mao Y Y, Gu L, Wang Y W and Peng X S 2013 CuO nanosheets/rGO hybrid lamellar films with enhanced capacitance *Nanoscale* **5** 9134–40
[28] Qian T, Yu C F, Wu S S and Shen J A 2013 Facilely prepared polypyrrole–reduced graphene oxide composite with a crumpled surface for high performance supercapacitor electrodes *J. Mater. Chem.* A **1** 6539–42

[29] Qian T, Zhou X, Yu C F, Wu S S and Shen J 2013 Highly dispersed carbon nanotube/polypyrrole core/shell composites with improved electrochemical capacitive performance *J. Mater. Chem.* A **1** 15230–4
[30] Dubal D P, Gund G S, Holze R, Jadhav H S, Lokhande C D and Park C J 2013 Surfactant-assisted morphological tuning of hierarchical CuO thin films for electrochemical supercapacitors *Dalton Trans.* **42** 6459–67
[31] Qian Y, Liu R, Wang Q F, Xu J, Chen D and Shen G Z 2014 Efficient synthesis of hierarchical NiO nanosheets for high-performance flexible all-solid-state supercapacitors *J. Mater. Chem.* A **2** 10917–22
[32] Dubal D P, Gund G S, Holze R and Lokhande C D 2013 Mild chemical strategy to grow micro-roses and micro-woolen like arranged CuO nanosheets for high performance supercapacitors *J. Power Sources* **242** 687–98
[33] Si P, Ding S J, Lou X W and Kim D H 2011 An Electrochemically formed three-dimensional structure of polypyrrole/graphene nanoplatelets for high-performance supercapacitors *RSC Adv.* **1** 1271–8
[34] Deng M J, Wang C C, Ho P J, Lin C M, Chen J M and Lu K T 2014 Facile electrochemical synthesis of 3D nanoarchitectured CuO electrodes for high performance supercapacitors *J. Mater. Chem.* A **10** 1039–46
[35] Yang P H *et al* 2013 Hydrogenated ZnOCoreShell nanocables for flexible supercapacitors and self-powered systems *ASC Nano* **7** 2617–26
[36] Liu J P, Jiang J, Bosman M and Fan H J 2012 Three-dimensional tubular arrays of MnO_2–NiO nanoflakes with high areal pseudocapacitance *J. Mater. Chem.* A **22** 2419–28
[37] Kim Y J, Abe Y, Yanagiura T, Park K C, Shimizu M, Iwazaki T, Nakagawa S, Endo M and Dresselhaus M S 2007 Easy preparation of nitrogen-enriched carbon materials from peptides of silk fibroins and their use to produce a high volumetric energy density in supercapacitors *Carbon* **45** 2116–25
[38] El-Kady M F, Strong V, Dubin S and Kaner R B 2012 Laser scribing of high-performance and flexible graphene-based electrochemical capacitors *Science* **335** 1326–30
[39] El-Kady M F and Kaner R B 2013 Scalable fabrication of high-power grapheme micro-supercapacitors for flexible and on-chip energy storage *Nat. Commun.* **4** 1475
[40] Ghaffari M, Zhou Y, Xu H, Lin M, Kim T Y, Ruoff R S and Zhang Q M 2013 High-volumetric performance aligned nano porous microwave exfoliated graphite oxide-based electrochemical capacitors *Adv. Mater.* **25** 4879–85
[41] Wu Z S, Parvez K, Winter A, Vieker H, Liu X J, Han S, Turchanin A, Feng X L and Müllen K 2014 Layer-by-layer assembled heteroatom-doped graphene films with ultrahigh volumetric capacitance and rate capability for micro-supercapacitors *Adv. Mater.* **26** 4552–8
[42] Yang Y, Ruan G D, Xiang C S, Wang G and Tour J M 2014 Flexible three-dimensional nanoporous metal-based energy devices *J. Am. Chem. Soc.* **136** 6187–90
[43] Yu D S, Goh K L, Wang H, Wei L, Jiang W C, Zhang Q, Dai L M and Chen Y 2014 Scalable synthesis of hierarchically structured carbon nanotube–graphene fibres for capacitive energy storage *Nat. Nanotechnology* **9** 555–62
[44] Yang W L, Gao Z, Ma J, Zhang X M, Wang J and Liu J Y 2014 Hierarchical NiCo2O4@NiO core–shell heterostructured nanowire arrays on carbon cloth for a high-performance flexible all-solid-state electrochemical capacitor *J. Mater. Chem.* A **2** 1448–57
[45] Qian Y, Liu R, Wang Q F, Xu J, Chen D and Shen G Z 2014 Hierarchical NiCo2O4@NiO core–shell heterostructured nanowire arrays on carbon cloth for a high-performance flexible all-solid-state electrochemical capacitor *J. Mater. Chem.* A **2** 1448–57
[46] Qian T, Xu N, Zhou J Q, Yang T Z, Liu X J, Shen X W, Liang J Q and Yan C L 2015 Interconnected three-dimensional V_2O_5/polypyrrole network nanostructures for high performance solid-state supercapacitors *J. Mater. Chem.* A **3** 488–93